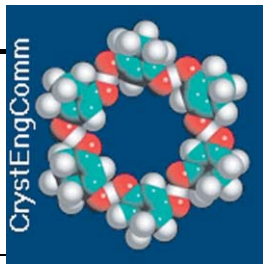

The first supramolecular architectures assembled by infinite hydrogen-bonded, protonated nucleobase–water ribbons and unusual polyiodide frameworks

Paper

Zheming Wang, Yajun Cheng, Chunsheng Liao and Chunhua Yan*

State Key Laboratory of Rare Earth Materials Chemistry and Applications, PKU-HKU Joint Laboratory on Rare Earth Materials and Bioinorganic Chemistry, Peking University-Nonius B. V. Demo Laboratory for X-Ray Diffraction, Peking University, Beijing 100871, China. E-mail: chyan@chem.pku.edu.cn

Received 16th October 2001, Accepted 2nd November 2001
Published on the Web 23rd November 2001

The crystal structures of $[AdeH^+](I_3^-)(I_2)_{5/2}(H_2O)$ and $[CytH^+]_2(I_5^-)_2(H_2O)_3$, where Ade is adenine and Cyt cytosine, are reported. The two compounds are the first examples of supramolecular architectures assembled from protonated nucleobases and polyiodides. In $[AdeH^+](I_3^-)(I_2)_{5/2}(H_2O)$, the mono-protonated adenine cations and water form hydrogen-bonded ribbons of nanometer width. The ribbons are embedded into a novel polyiodide matrix constructed by unusual rotaxane-like polyiodide chains. In $[CytH^+]_2(I_5^-)_2(H_2O)_3$, hydrogen-bonded cytosinium–water ribbons and polyiodide ribbons of combined branched polyiodide chains build a sheet-like structure containing alternately arranged positive and negative strips. Both architectures show good complementarity between the protonated nucleobase–water ribbons and polyioide species. The hydrogen bonds between the counter charged parts play a key role in stabilizing the associations.

Introduction

In past few years supramolecular architectures built by organic or inorganic cations and polyiodides have attracted much attention due to their richness in structural chemistry and supramolecular chemistry in particular.[1–14] In these architectures, the polyiodide species show not only a wide diversity in their geometrical features, from discrete oligomeric anions to variously extended 1D, 2D and 3D networks, but also an unusually continuous spectrum of I···I distances, from *ca.* 2.7 Å of the I_2 moiety to *ca.* 4 Å of the van der Waals radius summation of iodine, indicating the varying strengths of I···I interactions.[1–3] It has also been found that the formation and topology of polyiodide species depends on the nature, such as shape, size and charge, of the counter-cations; therefore the cations are usually considered as templating agents.[1,3] Besides the unconventional structural features and supramolecularity of polyiodides, the architectures display rich, complicated and fascinating intermolecular interaction patterns such as hydrogen bonds (both conventional and weak), π–π interactions, embraces, and the complementarity between cations and polyiodide anions.[4–9]

Many types of cations, transition metal complexes,[2,5–9] macrocyclothiother complexes,[1,3,4] organometallics[10,11] and nitrogen bases[12,13] have been used. Protonated nucleobases such as adenine (Ade) **1** or cytosine (Cyt) **2** (Chart 1), however, have never been explored before in this field. Nucleobases can be protonated and thus form various cations.[15–22] They possess multi-hydrogen-bonding sites and various tautomers[15] such that they can form an abundance of aggregates through hydrogen bonds, from dimers[15] (*e.g.* the well-known Watson–Crick pairs) to infinite extended species.[16,17,20–22]

The ability to form hydrogen-bonded networks is obviously the most important and interesting characteristic for nucleobases, because the self-assembly of hydrogen-bonded networks of nucleobases or their derivatives has been used to design or construct highly ordered supramolecular nanostructures, not only in 3D crystals[17,18,20] but also on 2D solid surfaces,[23,24] and these ordered nanostructures are of interest for their potential applications as molecular devices.[23,25] Finally, nucleobases are planar and aromatic, and therefore they should be suitable for intermolecular stacking and π–π interactions, and have complementarity with polyiodide species like other common aromatic nitrogen bases.[2,5–9] Thus, nucleobases should be expected to act as an interesting and unique class of templates comparable with other templating agents used in the construction of novel assemblies with polyiodides. As the first result of our systematic investigation on designing and constructing these assemblies, we report here the crystal structures of $[AdeH^+](I_3^-)(I_2)_{5/2}(H_2O)$ **1** and $[CytH^+]_2(I_5^-)_2(H_2O)_3$ **2**. As far as we are aware, they are the first architectures built by protonated nucleobases and polyiodides, and both contain hydrogen-bonded ribbons of nucleobase and water, and highly unexpected polyiodide species.

Experimental

Crystallization

$[AdeH^+](I_3^-)(I_2)_{5/2}(H_2O)$ **1**: adenine (0.134 g, 0.99 mmol), KI (0.327 g, 1.97 mmol) and I_2 (0.500 g, 1.97 mmol) were added to a mixed solution of 15 ml ethanol, water and 1 ml saturated

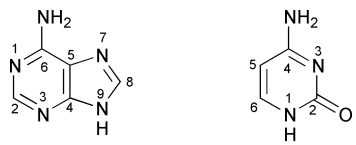

1 **2**

Chart 1 Molecular structure of adenine **1** and cytosine **2** with labeling of atomic sites. For adenine there are three N sites (1, 3 and 7) which can be protonated, and for cytosine only one N site (3) can be protonated.

hydrochloric acid. The solution was heated for 5 min and then filtered. Black columnar crystals (31 mg) were obtained by slow evaporation of the solvent at room temperature over several weeks. The product was soluble in DMF, methanol, THF, and acetonitrile, but insoluble in chloroform, cyclohexane, and n-heptane. IR (cm^{-1}, peaks of strong absorption only): 3089, 1688, 1614, 1446, 1395, 911, 891, 715, 619, 600, 556, 391, 164, 139.

$[CytH^+]_2(I_5^-)_2(H_2O)_3$ **2**: cytosine (0.060 g, 0.54 mmol), KI (0.178 g, 1.07 mmol) and I_2 (0.128 g, 0.50 mmol) were added to a mixed solution of 7 ml water and 6 ml saturated hydrochloric acid to give black deposits. The black deposits were dissolved in a solution of anhydrous ethanol and then filtered. Red–brown block-shaped crystals (28 mg) were obtained by slow evaporation of the solvent at room temperature over several weeks. Elemental analysis: found: C 6.65, H 1.71, N 5.59; calc.: C 6.21, H 1.17, N 5.43%. The product was soluble in DMF, methanol, THF, and acetonitrile, but insoluble in chloroform, cyclohexane, and n-heptane. IR (cm^{-1}, peaks of strong absorption only): 3383, 3150, 3112, 3072, 1720, 1673, 1664, 1543, 1230, 591, 566, 533, 419, 407, 167, 143, 88.

Crystallography

Both intensity data sets were collected at 293 K on a Nonius KappaCCD diffractometer with graphite-monochromated Mo Kα radiation ($\lambda = 0.71073$ Å). Cell parameters were obtained by the global refinement of the positions of all collected reflections. Intensities were corrected by Lorentz and polarization effects, and empirical absorption. Both structures were solved by direct methods, and refined by full-matrix, least squares on F^2 using the SHELX-97 package.[26] All non-H atoms were refined anisotropically. Locations of H atoms attaching to O and N were justified by difference Fourier synthesis. The H atoms of water in **1** and **2**, located from the difference Fourier synthesis, were refined using the ideal geometry of free water molecules, in which the O–H bond lengths were constrained at 0.96 Å and the H–O–H angle at 104.5°, as well as the same freely refined isotropic thermal factors, 0.12(3) $Å^2$ in **1** and 0.12(2) $Å^2$ in **2**. H atoms attaching to C and N were added geometrically and refined using the riding model. Details of crystallographic data for the structures are summarized in Table 1. Hydrogen bonds, both conventional and weak, are listed in Table 2 for **1**, and in Table 3 for **2**.

Table 1 Crystallographic data for **1** and **2**[a]

Parameter	**1**	**2**
Formula	$C_5H_8I_8N_5O$	$C_8H_{18}I_{10}N_6O_5$
Crystal dimensions/mm	0.25 × 0.20 × 0.17	0.20 × 0.15 × 0.09
M	1169.36	1547.28
Crystal system	Monoclinic	Triclinic
Space group	$P2_1/n$	$P\bar{1}$
a/Å	9.1467(2)	9.3062(2)
b/Å	24.7323(9)	13.2058(6)
c/Å	9.9400(4)	14.6192(6)
α/°	90	102.3835(16)
β/°	101.8877(17)	106.151(2)
γ/°	90	99.073(2)
V/$Å^3$	2200.39(13)	1639.72(11)
Z	4	2
D_c/g cm^{-3}	3.530	3.134
μ(Mo Kα)/mm^{-1}	11.277	9.475
$\theta_{min.}$, $\theta_{max.}$/°	3.40, 27.87	3.43, 27.88
Max., min. transmission	0.162, 0.111	0.445, 0.329
Extinction coefficient	0.00134(5)	0.00180(15)
Total reflections collected	23 535	28 976
Unique reflections (R_{int})	5221 (0.1151)	7749 (0.0515)
Observed reflections [$I \geqslant 2\sigma(I)$]	3460	5677
No. of refined parameters	180	304
Goodness of fit on F^2	1.041	1.054
R_1, wR_2 [$I \geqslant 2\sigma(I)$]	0.0398, 0.0769	0.0423, 0.0983
R_1, wR_2 (all data)	0.0758, 0.0868	0.0650, 0.1087
Max., min. residual density/e $Å^{-3}$	1.304, −1.062	1.180, −1.403
Max., mean shift/σ	0.000, 0.000	0.001, 0.000

[a]Click here for full crystallographic data (CCDC 163721 and 163722).

Results

Crystal structure of $[AdeH^+](I_3^-)(I_2)_{5/2}(H_2O)$ 1

In the structure the adenine molecule is mono-protonated at the N1 site, and the other protonated site is N7 (Fig. 1) instead of the usual N9 site for the neutral adenine (Chart 1), while N3 and N9 sites are not protonated. The larger internal ring C–N–C angle at N1 [124.0(6)°] than N3 [112.6(6)°] and also at N7 [106.5(5)°] than N9 [102.8(6)°] also confirm the protonation status.[15,17] The adenine cations form a positive ribbon (Fig. 1) through a pair of conventional inter-base N–H···N hydrogen bonds, N1–H···N9 and N6–H···N3 (Table 2). This hydrogen bonding pattern, resulting from the non-protonated N9 site, has never been described in any reported structure of adenine or its derivatives.[15–17,20,21] The two remaining N–H groups of the cation form two N–H···O hydrogen bonds (Table 2) with a peripheral water molecule. According to Etter's graph set theory for encoding hydrogen bonds,[27,28] the two hydrogen-bond patterns above described in the ribbon can be designated $R_2^2(8)$ and $R_2^1(7)$, respectively. These hydrogen bonds construct a positive adeninium–water ribbon. The ribbon has a width of *ca.* 1.0 nm with water molecules on the both sides. The ribbon runs along the [101] direction, the *ac* diagonal direction in the lattice.

The polyiodide species in the architecture displays very unusual and unexpected topological features described below. As shown in Fig. 2, four I_2 molecules (I5–I6, I7–I8, I5B–I6B and I7B–I8B) and two nearly linear and symmetric I_3^- anions (I2–I3–I4 and I2B–I3B–I4B) form a chair-ring-like I_{14}^{2-} anion of centric symmetry.

The foot and head of the chair are composed of two connected I_2 molecules in a V shape, and they are linked by two parallel I_3^- anions. These chairs are further connected by another type of I_2 molecule (I1–I1A in Fig. 2) lying on the inversion center, which connects two I_3^- anions of adjacent chairs, leading to the formation of a one-dimensional chain (Fig. 2). The $I_2\cdots I_3^-$ and $I_2\cdots I_2$ interactions involved in the chain are quite strong considering that these I···I distances are in the range 3.27–3.63 Å, and these values indicate rather strong I···I interactions or bonding[1,2] among I_2 and I_3^- moieties in the chain. Furthermore, two chains interpenetrate

Table 2 Geometry of hydrogen bonds in **1**

D–H···A	d(D–H)/Å	d(H···A)/Å	d(D···A)/Å	∠(DHA)/°
N(7)–H(7)···O(1)	0.86	2.06	2.841(8)	151.5
N(1)–H(1)···N(9)$^{\#1}$	0.86	1.93	2.786(8)	174.1
N(6)–H(61)···N(3)$^{\#1}$	0.86	2.13	2.983(8)	173.6
N(6)–H(62)···O(1)	0.86	2.12	2.953(7)	162.0
O(1)–H(11)···I(7)$^{\#2}$	0.95(2)	2.98(5)	3.745(6)	139(6)
O(1)–H(11)···I(3)$^{\#2}$	0.95(2)	3.11(6)	3.792(5)	130(5)
O(1)–H(12)···I(4)$^{\#2}$	0.95(2)	3.28(5)	4.117(5)	147(5)
O(1)–H(12)···I(1)$^{\#3}$	0.95(2)	3.35(10)	3.758(6)	108(7)
O(1)–H(12)···I(2)$^{\#4}$	0.95(2)	3.59(10)	3.691(6)	89(6)
C(2)–H(2)···I(2)$^{\#1}$	0.93	3.47	4.261(7)	144.6
C(2)–H(2)···I(3)$^{\#1}$	0.93	3.16	3.866(7)	134.0
C(2)–H(2)···I(8)$^{\#5}$	0.93	3.44	3.810(7)	106.4
C(8)–H(8)···I(1)$^{\#3}$	0.93	3.28	3.887(7)	124.4
C(8)–H(8)···I(7)$^{\#3}$	0.93	3.52	3.859(7)	104.3
N(7)–H(7)···I(1)$^{\#3}$	0.86	3.33	3.869(5)	123.2

Symmetry transformations used to generate equivalent atoms: #1 $x + 1/2, -y + 1/2, z + 1/2$; #2 $-x + 1, -y, -z$; #3 $-x, -y, -z$; #4 $x + 1, y, z + 1$; #5 $-x + 1/2, y + 1/2, -z + 1/2$.

Table 3 Geometry of hydrogen bonds in **2**

D–H···A	*d*(D–H)/Å	*d*(H···A)/Å	*d*(D···A)/Å	∠(DHA)/°
N(11)–H(11)···O(3)$^{\#1}$	0.86	2.04	2.887(7)	169.2
N(13)–H(13)···O(4)	0.86	1.93	2.753(7)	158.5
N(14)–H(141)···O(3)	0.86	2.30	3.062(8)	147.5
N(21)–H(21)···O(5)$^{\#1}$	0.86	2.10	2.942(8)	164.9
N(23)–H(23)···O(12)	0.86	1.85	2.677(7)	159.9
N(24)–H(241)···O(12)	0.86	2.29	2.995(8)	139.4
N(24)–H(241)···O(4)	0.86	2.58	3.252(9)	135.3
N(24)–H(242)···O(5)	0.86	2.18	3.004(8)	159.1
O(3)–H(32)···O(22)$^{\#2}$	0.95(2)	1.96(4)	2.875(7)	161(9)
O(4)–H(41)···O(22)$^{\#2}$	0.95(2)	1.82(2)	2.775(7)	176(8)
O(3)–H(31)···I(1)$^{\#3}$	0.95(2)	2.98(5)	3.810(6)	146(6)
O(3)–H(31)···I(5)$^{\#4}$	0.95(2)	3.18(7)	3.784(5)	123(6)
O(4)–H(42)···I(9)$^{\#5}$	0.96(2)	2.77(4)	3.665(7)	155(7)
O(4)–H(42)···I(10)$^{\#5}$	0.96(2)	2.71(5)	3.557(18)	147(6)
O(5)–H(51)···I(3)$^{\#4}$	0.96(2)	3.10(8)	3.727(7)	124(7)
O(5)–H(52)···I(8)$^{\#5}$	0.96(2)	2.93(7)	3.714(7)	140(8)
C(15)–H(15)···I(8)	0.93	3.15	3.935(7)	143.6
C(15)–H(15)···I(6)$^{\#2}$	0.93	3.27	4.078(7)	146.1
C(16)–H(16)···I(7)	0.93	3.36	4.275(6)	167.1
N(14)–H(142)···I(6)$^{\#2}$	0.86	3.03	3.855(6)	161.1
C(25)–H(25)···I(3)$^{\#2}$	0.93	3.37	4.294(6)	174.8
C(26)–H(26)···I(1)	0.93	3.14	3.910(7)	142.0
C(26)–H(26)···I(2)	0.93	3.33	4.244(7)	166.4
O(5)–H(51)···I(3)$^{\#2}$	0.96(2)	3.06(6)	3.795(6)	135(6)

Symmetry transformations used to generate equivalent atoms: #1 $x-1, y, z$; #2 $x+1, y, z$; #3 $x+1, y+1, z$; #4 $-x-1, -y-1, -z$; #5 $x, y-1, z$.

with each other, giving a one-dimensional rotaxane-like structure (Fig. 3). The interchain I···I separations are larger than 4.0 Å, indicating very weak I···I interchain interactions.[1] Each linkage I_2 molecule in one chain is clamped by, and is coplanar with, the two I_3^- moieties of one chair I_{14}^{2-} anion of the other chain. This rotaxane-like chain is the most striking feature in the architecture, because an entangled polyiodide

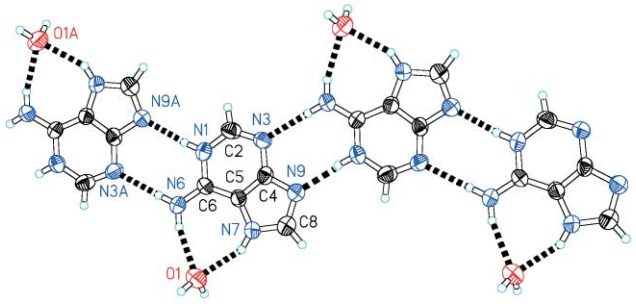

Fig. 1 Ortep drawing of the positive ribbon composed by monoprotonated adenine cations and water molecules through hydrogen bonds (dashed solid bonds) in **1**. Hydrogen bonds are: N–H···N 2.786(8), 2.983(8) Å; N–H···O 2.953(7), 2.841(8) Å. The ribbon runs along the *ac* diagonal direction. Symmetry code: A $x+1/2, -y+1/2, z+1/2$. Click image or here to access a 3D representation.

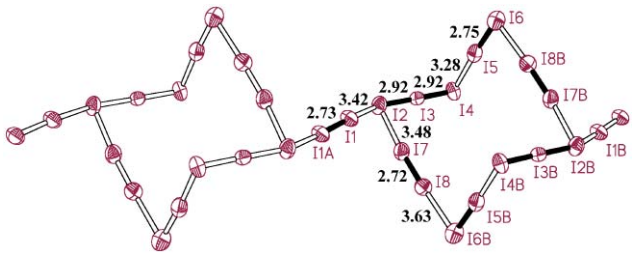

Fig. 2 Polyiodide chain formed by I_2 linking chair-like I_{14}^{2-} anions in **1**, showing atomic labeling scheme and I–I distances. Some I_2 and I_3^- units are highlighted by solid bonds. Symmetry codes: A $-1-x, -y, -z$; B $1-x, -y, -z$.

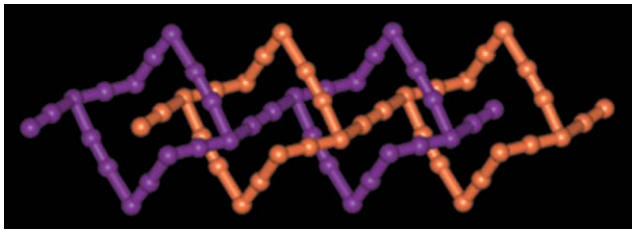

Fig. 3 Rotaxane-like polyiodide chain in **1**. The two individual chains interpretrating with each other are colored purple and orange.

chain has never been observed previously though the chair-ring-like polyiodide species and different linking styles of these chairs have never been described before.[7,12,13,29]

In the previously reported results, adjacent polyiodide chair-rings are either linked by chains of alternating I^- and I_2 directly into layers,[7] or they are connected by single or double I_2 bridges to form 1D chains or ribbons, which are further linked to generate layers.[13] Polyiodide chairs can also adopt the direct-linking or edge-sharing style to form layer structures.[12,29] These rotaxane-like chains are juxtaposed *via* weak I···I contacts, with the shortest I···I distance of 3.94 Å, to form a layer (Fig. 4) with sawtooth-like lines, which are built by the V-shaped feet and heads of the chair-ring I_{14}^{2-} anions, on both sides. Finally, when these polyiodide layers stack into a 3D structure (Fig. 5), the sawtooth-like lines of the neighboring layers interdigitate together, yielding an interesting polyiodide

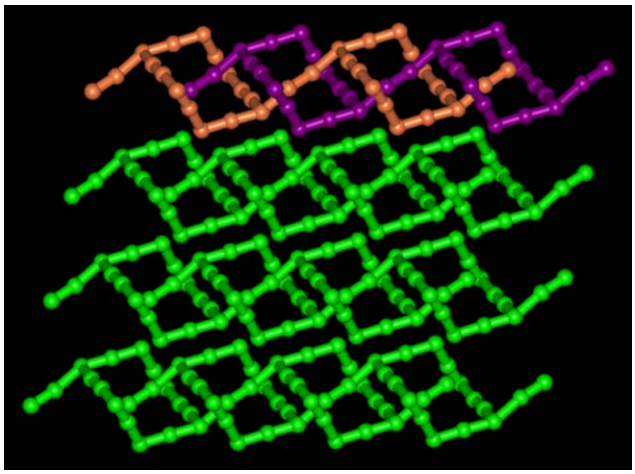

Fig. 4 Layer composed by juxtaposed rotaxane-like polyiodide chains in **1**. One rotaxane chain is highlighted by purple and orange colors. The sawtooth-like lines run from top-left to bottom-right on both sides of the layer in this figure.

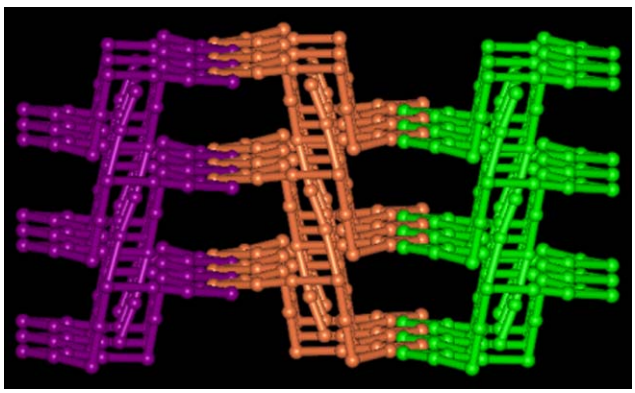

Fig. 5 Polyiodide matrix formed by the three interdigitated layers (purple, orange and green), displaying the rectangular channels formed by the interclocking of layers. The view is roughly along the *ac* diagonal direction.

framework, which contains channels of roughly rectangular profile of dimensions *ca.* 1.1 × 0.7 nm. The slightly bent top and bottom of the channel are the interlocked sawtooth-like lines, whereas the side walls are made up of the middle parts of the entangled chains. The interdigitation of polyiodide layers has rarely been observed before.

In the lattice, the channels of the polyiodide matrix run along the *ac* diagonal direction, and are occupied by the positive adeninium–water ribbons (Figs. 6 and 7). The ribbon fits the polyiodide channel well. It is slightly bent and nearly parallel to the top and bottom of the channel. The top and the bottom of the channel are *ca.* 3.7 Å above or below the ribbon. In the interfacial region between the ribbon and polyiodide side wall (Fig. 7), the water molecules of the positive ribbons are, in fact, inserted into the sides of the channels, and form O–H···I hydrogen bonds (O···I distances *ca.* 3.69–4.12 Å) with the polyiodide framework (Fig. 7). The I_2 and I_3^- segments of the wall show complementary orthogonality[5,6] to the adeninium cations. The C–H and N–H weak donors of adeninium form weak C–H···I and N–H···I hydrogen bonds[2,5–8,30] of C/N···I distances *ca.* 3.81–3.89 Å with the polyiodide matrix. These hydrogen bonds (Table 2), together with the electrostatic and π–π interactions between the positive ribbons and the negative polyiodide channels, contribute to the stabilization of the novel and interesting supramolecular assembly. This association, therefore, shows good complementarity between the adeninium–water ribbons and the polyiodide matrix.

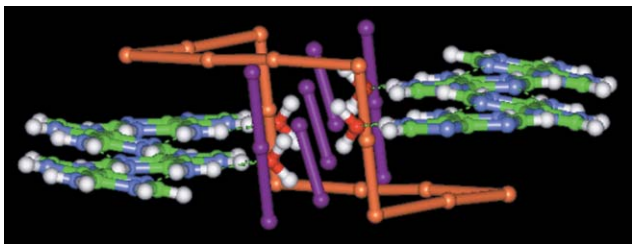

Fig. 6 Adeninium–water ribbons embedded in the rectangular channels. Only part of the polyiodide matrix, the side wall between two adjacent polyiodide channels, is shown here. One I_{14}^{2-} chair-ring is colored orange.

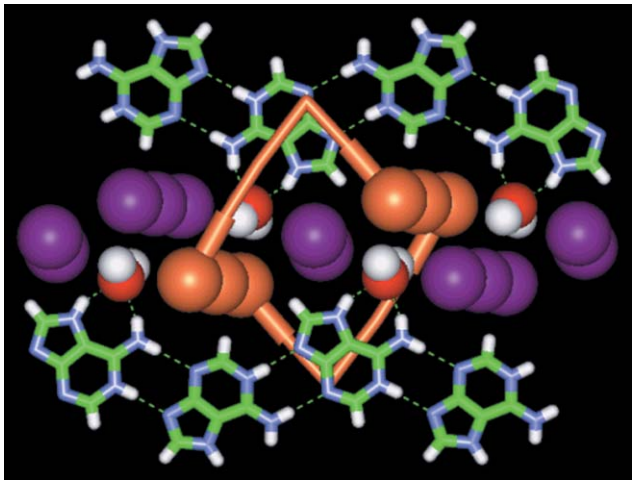

Fig. 7 Top view of Fig. 6, showing the interfacial interaction between the adeninium–water ribbon and the side of the polyiodide channel. Oxygen atoms of water are represented by red spheres. Large purple and orange spheres represent the iodine atoms of I_2 and I_3^- moieties constructing the side-wall of the polyiodide channel. They are nearly orthogonal and peripheral to the adeninium cations. The head and the foot parts of one I_{14}^{2-} chair, colored orange, are shown in stick style for clarity.

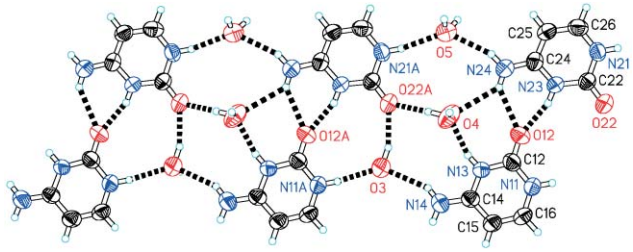

Fig. 8 Ortep plot of the cytosinium–water ribbon in **2**, viewed roughly along the *c* axis, with atomic labels and hydrogen bonds (dashed solid bonds) shown. Within the positive ribbon the N···O distances of the N–H···O hydrogen bonds are in the range *ca.* 2.68–3.25 Å, and the O···O distances of the O–H···O hydrogen bonds *ca.* 2.78–2.88 Å. Symmetry code: A $x + 1$, y, z.

Crystal structure of $[CytH^+]_2(I_5^-)_2(H_2O)_3$ 2

The crystal structure of **2** (Figs. 8–10) consists of sheets assembled by alternately arranged positive $\{[CytH^+]_2(H_2O)_3\}_n$ ribbons and negative $[(I_5^-)_2]_n$ polyiodide ribbons. We first describe the ribbons and then their association in the structure.

As shown in Fig. 8, in the positive ribbon two protonated cytosine cations, whose protonation status is also justified by the larger internal ring C–N–C angles [122.4(5)–125.4(5)°] at

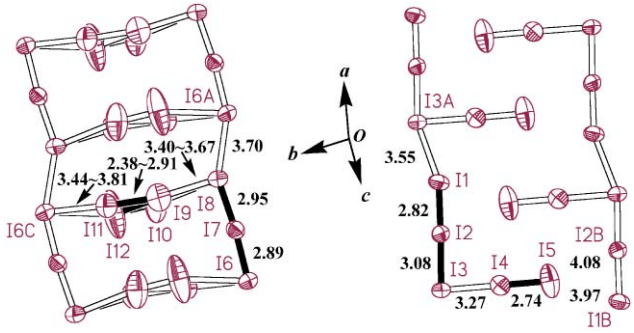

Fig. 9 Two independent polyiodide ladder-like ribbons in **2**, with atomic labeling scheme and I–I distances. The I–I bonds of some I_2 and I_3^- moieties are highlighted by solid bonds. Symmetry codes: A $x + 1$, y, z; B $-x - 2$, $-y - 2$, $-z$; C $-x$, $-y + 2$, $-z + 1$.

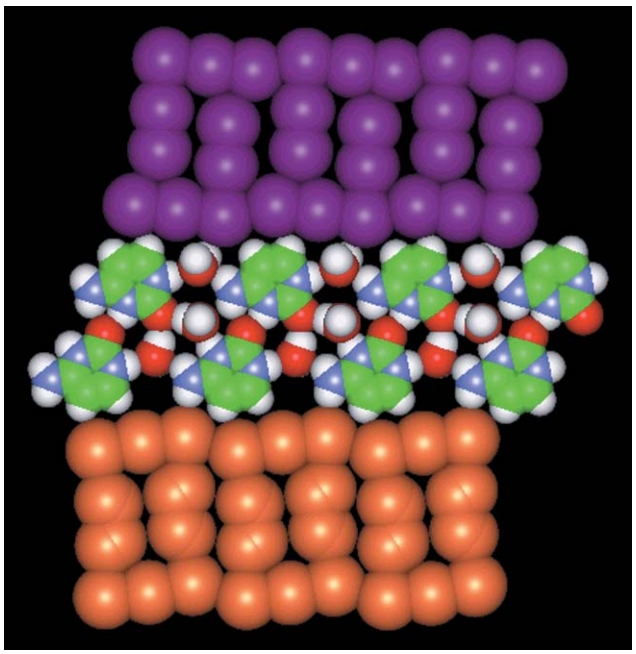

Fig. 10 One sheet composed of alternately arranged negative and positive ribbons in **2**, viewed roughly along the *c* axis. Colors scheme: I purple and orange; O red; N blue; C green; H white.

the ring N sites,[15,22] form a bifurcated acceptor type of hydrogen bond $(N–H)_2\cdots O$ between the O acceptor of one cytosinium and two N–H donors of another cytosinium. Between the adjacent cytosinium pairs there are three water molecules. They act as hydrogen-bond connectors to link the cytosinium pairs through several N–H···O and O–H···O hydrogen bonds (Table 3), and thus build the hydrogen-bonded and nearly planar ribbon of width *ca.* 1.0 nm. In the ribbon the hydrogen-bonding patterns exhibit four or five different ring types, and include several types of bifurcated hydrogen bond, $(O–H)_2\cdots O$, $(N–H)_2\cdots O$ and $N–H\cdots(O)_2$ (Fig. 8). The occurrence of the bifurcated hydrogen bonds is in agreement with the fact that protonated cytosine is donor-rich because each cytosinium has four N–H donors but only one O acceptor, and is found in other cytosine structures.[22]

The negative ribbons of this structure are two crystallographically independent polyiodide ladders (Fig. 9), composed of asymmetric and slightly bent I_3^- anions and I_2 molecules. In one polyiodide ladder all positions of the iodine atoms (I1 to I5) are ordered, whereas in another ladder the I_2 (I9 to I12) molecules are slightly disordered. The side-pieces of the ladder are built by end-to-end-connected I_3^- anions whereas the rungs are made up of I_2 molecules. This ladder can also be described as the interlock of two branched chains of linking L- (or V-) shaped I_5^- anions of opposite orientation. The branched chains of the polyiodide are rarely observed because L- (or V-) shaped I_5^- anions typically form the long-known zigzag chains.[31] The ladder is structurally different from the reported one[32] in which the branched chain has the main part being I_3^- – end-connected I_2 molecules and branches being the other two iodine atoms of the I_3^- anion. Fig. 9 gives the I–I bond distances in the two independent polyiodide ladders. The disordered I_2 leads to a somewhat larger diversity of I–I bond distances.

Both positive and negative ribbons are of almost the same width, *ca.* 1.0 nm, and thus they are complementary to each other in shape and size. They form sheet-like structures in which the positive and negative ribbons are alternately arranged, side by side, along the sheet plane (Fig. 10). Numerous weak N–H···I and C–H···I hydrogen bonds[5–8,30] (Table 3) between the counter-charged ribbons interweave these ribbons. The hydrogen bond distances between the positive and negative ribbons are C···I ≈ 3.91–4.29 Å and N···I 3.86 Å, respectively. These sheets stack along the *c* direction and form a 3D architecture through the electrostatic and π–π interactions between the counter-charged ribbons. The inter-sheet separation is *ca.* 3.6 Å. The positive ribbon in one sheet is clamped by two negative ribbons of the adjacent two sheets, so that each positive ribbon is, in fact, surrounded by four negative polyiodide ribbons, and *vice versa*. In the 3D architecture, the remaining O–H donors of water molecules form O–H···I-type hydrogen bonds between the sheets, with O···I distances of 3.56–3.81 Å, giving extra stabilization to the architecture.

Discussion

The two compounds are the first examples of supramolecular architectures assembled from protonated nucleobases and polyiodides. Both have unique hydrogen-bonded nucleobase–water ribbons and unusual polyiodide species of combined rotaxane-like or branched chains, and display fascinating architectures through hydrogen bonds and good complementarity between two counter-charged parts. In the first structure the adeninium–water ribbons, of width *ca.* 1 nm, are embedded in a 3D polyiodide matrix, whereas in the second, cytosinium–water ribbons and polyiodide ribbons, both of nanosized width, form sheets containing alternately arranged positive and negative strips. Therefore, both architectures are nanosized supramolecular structures, which may be of future interest, for designing and building molecular devices such as electron or proton nanowires,[23,25] or for their anisotropically electrical properties.[32,33]

Nucleobases, either protonated or non-protonated, have multi-hydrogen-bonding sites of special geometry arrangements such that they have the great tendency to form extended aggregates[16,17,20–22] through hydrogen bonds, like the nucleobase–water ribbons described above. This is obviously the major difference of nucleobases from other cations, which are usually considered to be discrete templates. On the other hand, this work shows that the inter-base hydrogen-bonding seems not to be interrupted by polyiodide. This is probably because the formation of strong N–H···N, N–H···O and O–H···O hydrogen bonds is more favorable than the formation of weak N–H···I, O–H···I and C–H···I hydrogen bonds. The C–H donors of the nucleobase are also suitable for weak C–H···I hydrogen bonds.[4–8] Therefore, the use of these hydrogen-bonded templates will allow new polyiodides of different and unexpected composition and topology to be obtained, leading to novel supramolecular architectures. Further study by using various aggregates of nucleobases as templates to build supramolecular architectures with polyiodides, for instance, embedding the well-known Watson–Crick pairs into the polyiodide matrix, can be expected and is of merit to carry out. It is also naturally suggestive to extend the study to the nucleobase derivatives. We think that this paper will initiate the related studies.

Acknowledgements

This work was supported by MOST of China (No. G1998061310), NSFC (Nos. 29831010 and 20023005) and the Founder Foundation of Peking University.

References

1 A. J. Blake, F. A. Devillanova, R. O. Gould, W.-S. Li, V. Lippolis, S. Parsons, C. Radek and M. Schröder, *Chem. Soc. Rev.*, 1998, **27**, 195 and references therein.
2 C. Horn, M. Scudder and I. Dance, *CrystEngComm*, 2001, **2**.
3 S. Menon and M. V. Rajasekharan, *Inorg. Chem.*, 1997, **36**, 4983.
4 A. J. Blake, R. O. Gould, W.-S. Li, V. Lippolis, S. Parsons, C. Radek and M. Schröder, *Angew. Chem., Int. Ed.*, 1998, **37**, 293.
5 C. Horn, M. Scudder and I. Dance, *CrystEngComm*, 2001, **1**.
6 C. Horn, B. Ali, I. Dance, M. Scudder and D. Craig, *CrystEngComm*, 2000, **2**.
7 C. Horn, M. Scudder and I. Dance, *CrystEngComm*, 2000, **9**.
8 C. Horn, M. Scudder and I. Dance, *CrystEngComm*, 2000, **36**.
9 Z.-M. Wang, M. Yan, Z. He, C.-S. Liao and C.-H. Yan, *Acta Chim. Sin.*, 2000, **58**, 1615.
10 K.-F. Tebbe and R. Buchem, *Angew. Chem., Int. Ed. Engl.*, 1997, **36**, 1345.
11 K.-F. Tebbe and R. Buchem, *Z. Anorg. Allg. Chem.*, 1998, **624**, 671.
12 R. Loukili and K.-F. Tebbe, *Z. Anorg. Allg. Chem.*, 1999, **625**, 650.
13 K.-F. Tebbe and R. Loukili, *Z. Anorg. Allg. Chem.*, 1998, **624**, 1175.
14 K.-F. Tebbe and M. Bittner, *Z. Anorg. Allg. Chem.*, 1995, **621**, 218.
15 W. Saenger, *Principles of Nucleic Acid Structure*, Springer-Verlag New York Inc., New York, 1984, ch. 4–6.
16 J. Jai-nhuknan, A. G. Karipides and J. S. Cantrell, *Acta Crystallogr., Sect. C*, 1997, **53**, 454.
17 A. C. M. Young, J. C. Dewan and A. J. Edwards, *Acta Crystallogr., Sect. C*, 1991, **47**, 580.
18 J. Maixner and J. Zachova, *Acta Crystallogr., Sect. C*, 1991, **47**, 2474.
19 P. de Meester and A. C. Skapski, *J. Chem. Soc., Dalton Trans.*, 1973, 1596.
20 T. J. Kistenmacher and T. Shigematsu, *Acta Crystallogr., Sect. B*, 1974, **30**, 166.
21 T. J. Kistenmacher and T. Shigematsu, *Acta Crystallogr., Sect. B*, 1974, **30**, 1528.

22 N. S. Mandel, *Acta Crystallogr., Sect. B*, 1977, **33**, 1079.
23 G. Gottarelli, S. Masiero, E. Mezzina, S. Pieraccini, J. P. Rabe, P. Samori and G. P. Spada, *Chem. Eur. J.*, 2000, **6**, 3242.
24 S. J. Sowerby, M. Edelwirth and W. M. Heckl, *J. Phys. Chem. B*, 1998, **102**, 5914.
25 J. M. Lehn, *Supramolecular Chemistry*, VCH, Weinheim, 1995, p. 121.
26 G. M. Sheldrick, SHELX-97, Program for Crystal Structure Determination, University of Göttingen, Germany, 1997.
27 M. C. Etter, *Acc. Chem. Res.*, 1990, **23**, 120.
28 J. Bernstein, R. E. Davis, L. Shimoni and N.-L. Chang, *Angew. Chem., Int. Ed. Engl.*, 1995, **34**, 1555.
29 P. H. Svensson, G. Raud and L. Kloo, *Eur. J. Inorg. Chem.*, 2000, **6**, 1275.
30 T. Steiner, *Acta Crystallogr., Sect. B*, 1998, **54**, 456.
31 T.-Y. Dong, M.-Y. Hwang, C.-C. Schei, S.-M. Peng and S.-K. Yeh, *J. Organomet. Chem.*, 1989, **369**, C33.
32 R. D. Bailey and W. T. Pennington, *Acta Crystallogr., Sect. B*, 1995, **51**, 810.
33 D. Ramalakshmi, K. R. Reddy, D. Padmavathy, M. V. Rajasekharan, N. Arulsamy and D. J. Hodgson, *Inorg. Chim. Acta*, 1999, **284**, 158.